Deployable Membrane Reflectors

S. Pellegrino

Department of Engineering, University of Cambridge
Trumpington Street, Cambridge, CB2 1PZ, U.K.
pellegrino@eng.cam.ac.uk

ABSTRACT: This paper is concerned with the design of a new type of multi-purpose deployable membrane reflector. The reflector structure consists of a central expandable hub, a number of thin-walled foldable ribs connected radially to the hub, and a precision-shaped membrane supported and tensioned by the ribs. This concept is known as a collapsible rib-tensioned surface reflector. A methodology for the design of reflectors of this type that meet specified requirements is presented; both offset and symmetric configurations can be designed. For a reflector aperture of 10 m diameter and a focal length of 7.8 m, a root-mean-square surface accuracy of about 2 mm is achievable; this result scales linearly with the diameter. The design of a 1.5 m diameter prototype is presented, and the accuracy and deployment behaviour of a physical model are measured experimentally.

INTRODUCTION

Large deployable reflectors are being used increasingly for satellite communication, radioastronomy and earth observation. The requirement for large apertures that can be compactly packaged for launch and reliably deployed in orbit, to achieve their intended configuration precisely, has spurred extensive new research worldwide. A new concept for multi-purpose deployable membrane reflectors is being developed by the European Space Agency (Rits 1996); this new concept is known as the *Collapsible Rib-Tensioned Surface (CRTS)* reflector.

This deployable reflector consists of three main parts. A central expandable hub, a number of thin-walled foldable ribs connected radially to the hub, and a precision shaped membrane that is supported and tensioned by the ribs.

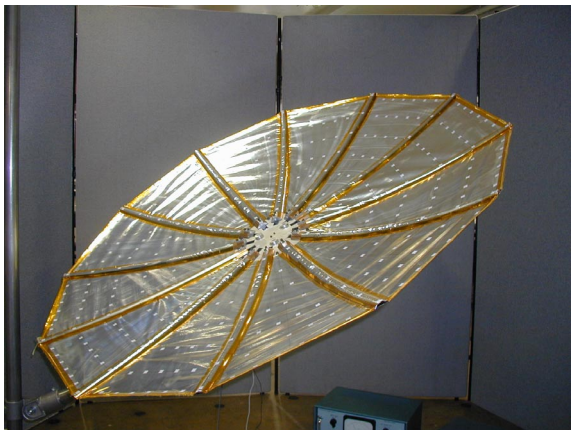

Figure 1: 1.5 m diameter model of CRTS reflector.

A photograph of a small-scale prototype is shown in Fig. 1. During deployment the hub is retracted to its largest radius configuration, so that the ribs can deploy the membrane without having to prestress it as well. After the membrane has been fully deployed, the hub is expanded, thus pushing the ribs radially outwards by a small amount. This has the effect of applying a state of prestress to the membrane, which sets it into its intended shape.

The shape of the reflector is required to be as close as possible to a perfect paraboloid. The accuracy of this approximation is related to the deviation of the surface from the best-fit paraboloid, and is usually measured in terms of an overall root-mean-square error, δ_{rms} (Levy, 1996). This value depends on both the number of ribs and the shape of the membrane between adjacent ribs.

The particular configuration of the CRTS reflector that is of greatest interest for communication satellites is known as *offset*, which means that the focal axis of the paraboloid does not pass through the centre of the hub.

This paper presents a methodology for the design of offset CRTS reflectors to meet a set of specified requirements; symmetric reflectors are also covered, as a special case. After briefly describing the geometry of offset reflectors, a procedure is given for determining the prestress distribution, the shape and corresponding accuracy of a particular design. In particular, a method is presented for prestressing the membrane without applying out-of-plane forces on the ribs, which is the major difficulty of offset reflector design. Then, the design of a 1.5 m diameter reflector is presented, and the accuracy and deployment behaviour of a physical prototype are measured experimentally.

Note that simple scaling arguments can be used to show that —first— the root-mean-square error, δ_{rms}, scales linearly with the aperture D of the reflector, and —second— the forces applied to the ribs and to the edge cords also scale linearly with D if the level of prestress is kept the same. Therefore, only reflectors with a particular aperture, $D = 10$ m, will be considered in this study, as the properties of any other size can be obtained by scaling.

OFFSET REFLECTORS

The standard way of defining the geometry of an offset reflector is to consider the intersection of a paraboloid with the required focal length, known as *parent paraboloid*, with a circular cylinder of diameter D, whose axis is parallel to the axis of the paraboloid (Levy, 1996). Figure 2 shows a three-dimensional view of an offset reflector with its parent paraboloid. To help visualize the shape of the reflector a series of ellipses have been drawn; these lines are obtained by intersecting the paraboloid with a series of coaxial circular cylinders. The outermost cylinder, defining the edge of the reflector, has radius $R_a = D/2$.

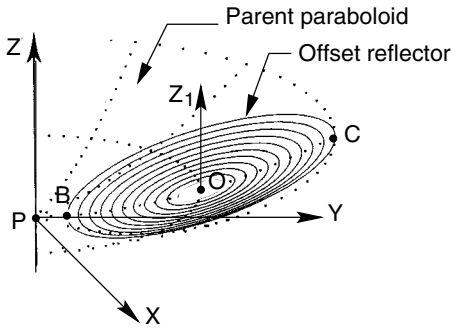

Figure 2: Three-dimensional view of standard offset reflector.

With reference to Fig. 3, consider an offset reflector with focal length F, offset Y_0 from the centre of the parent paraboloid to the centre of the aperture, and distance A from the focal axis of the parent paraboloid to the near side of the edge of the reflector. Its equation can be expressed in the local co-ordinate system X_L, Y_L, Z_L defined in Fig. 3, where the Y-coordinate of the origin O is normally given by $Y_0 = A + R_a$. With the notation $s = \sin\phi_a$ and $c = \cos\phi_a$, the equation of the offset reflector in the local coordinate system is

$$sY_L + cZ_L + Z_0 = \frac{1}{4F}[X_L^2 + (cY_L - sZ_L + Y_0)^2] \quad (1)$$

Figure 4(a) shows the intersections between the co-axial cylinders described above and the plane $X_L Y_L$. This standard configuration is unsuitable for CRTS reflectors, because it leads to poor prestress distributions in the membrane. Lai and Pellegrino (1999) have shown that the best configuration from the viewpoint of the prestress distribution, and hence of efficient structural design, is a configuration such that its projection onto the local plane is a circle, see Fig. 4(b).

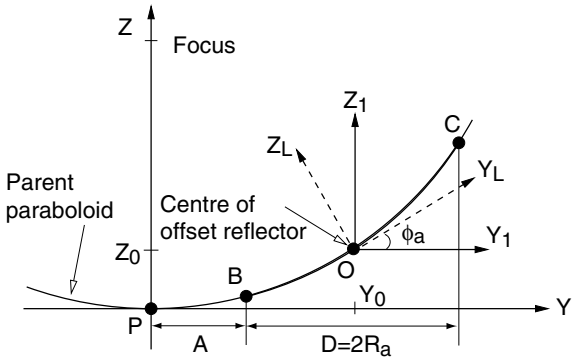

Figure 3: Definition of offset reflector.

Denoting by R_a the radius of the circle defined in Fig. 4(b), the Y-coordinate of the origin, O, in the global X, Y, Z coordinate system, Y_0, is found by considering point B in Figure 3. Then the Y-coordinate of B in the local coordinate system, Y_{BL}, is given by:

$$\begin{aligned} Y_{BL} &= cY_{B1} + sZ_{B1} \\ &= (Y_B - Y_0)\cos\tan^{-1}\frac{Y_0}{2F} \\ &\quad +(Z_B - Z_0)\sin\tan^{-1}\frac{Y_0}{2F} \end{aligned} \quad (2)$$

Also, from Fig. 4(b), $Y_{BL} = -R_a$, hence Equation 2 can be solved for the unknown Y_0.

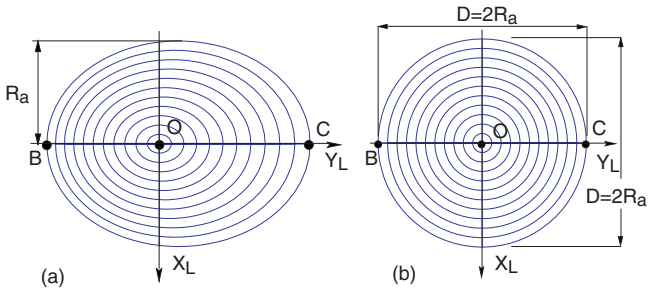

Figure 4: Projection onto local plane of (a) standard offset configuration and (b) "circular" offset configuration.

GENERAL DESIGN METHODOLOGY

To design a CRTS reflector we need to think about three theoretical surfaces, as follows.

1. The *reference surface* is the locally cylindrical surface defined by the parabolic ribs of the reflector. This surface is the best possible shape that can be achieved with a given number of ribs; to achieve it, we have to prestress the membrane purely in the hoop direction.

2. The *equilibrium surface* is any shape of the reflector in which an acceptable prestress distribution is in equilibrium. For any given prestress distribution, we can compute a corresponding equilibrium surface. If biaxial prestress is required, the equilibrium surface has to be locally doubly-curved; however if uniaxial prestress is acceptable, then the equilibrium surface coincides with the reference surface.

3. Finally, the *actual surface* is the expected shape of the reflector, which can be compared with measurements from the real structure. It is obtained by projecting the equilibrium surface onto flat pieces of membrane, which of course introduces some errors, and by computing the prestressed shape of the structure made by joining these pieces and pushing outwards the ribs.

For each of these surfaces, we can compute the equation of the best-fit paraboloid and hence the corresponding δ_{rms}. Typical results for a symmetric reflector ($A = 0$) and an offset reflector with offset $A = 1$ m are listed in Table 1.

Geometry	No. of ribs	δ_{rms} [mm]
Symmetric Configuration	6	39.6
	12	9.6
	24	2.4
Offset Configuration ($A = 1$ m)	6	45.9
	12	12.5
	24	3.3

Table 1: Typical surface errors of reflectors with $D = 10$ m and $F = 7.8$ m.

Given the aperture diameter, focal length, and target δ_{rms}, as well as the maximum permissible ratio between the highest and lowest principal stress in the membrane, the key stages of the design process are as follows.

1. Preliminary determination of required number of ribs, based on a purely geometric computation (reference surface).

2. Computation of an equilibrium surface which is sufficiently accurate, in tension everywhere, and such that the ratio between maximum and minimum stress is acceptable.

3. Computation of the cutting pattern.

4. Verification that the shape and prestress distribution in a membrane made from a series of linear-elastic gores cut according to the pattern computed above satisfies all the stated requirements.

5. Computation of the unstressed profile of the ribs.

The computations required to implement this design methodology are set out in Lai and Pellegrino (1998). The first step in the search for the equilibrium surface consists in choosing the particular prestress distribution that is desired.

The membrane is represented by a virtual, triangulated cable network, and the assigned prestress is transformed into equivalent cable forces; the key idea is illustrated in Fig. 5. Additional, real cable elements represent the cords along the edges of the gores.

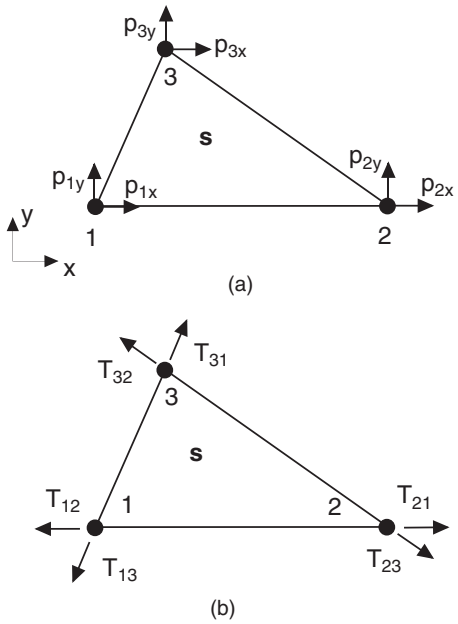

Figure 5: (a) Triangular element with constant prestress **s** and (b) equivalent cables with corresponding pretensions T_{ij}.

The initial nodal coordinates are defined by considering an equal number of equally spaced nodes on each rib. The membrane nodes are then defined to lie initially on straight lines between corresponding nodes of adjacent ribs, and hence their coordinates can be found by interpolation of the coordinates of the two rib nodes. Thus, the initial geometry of the reflector is the reference configuration.

To determine an equilibrium shape and the associated prestress distribution, one computes the ratio between the internal force in each cable and its length (force density). The equilibrium equations of the virtual cable structure yield a linear system of equations that are solved to find the nodal coordinates of the cable network. The positions of these nodes define a possible equilibrium surface for the reflector, and the corresponding δ_{rms} is computed. The associated principal stress components in each triangular element, which are different from those assumed at the start of the computation, are also computed. If the results of these computations are acceptable, the next stage of the computation finds the cutting pattern required to

make a prestressed membrane whose shape closely approximates to the equilibrium surface, out of flat gores. The prestressed shape of this membrane is then computed by means of an elastic finite element analysis, followed by a computation of the rms error of this surface. Finally, the unstressed rib profiles are computed.

A fuller description of the algorithm is available in Lai, You and Pellegrino (1998).

Prestressing an Offset Reflector

The key difference between symmetric and offset reflectors is that an offset reflector has only one plane of symmetry, $Y_L Z_L$, hence half of the whole surface needs to be considered in the analysis. In the case of axi-symmetric configurations only one gore needs to be analysed, as all gores have identical shape and prestress.

A significant challenge at this point is to obtain an initial prestress distribution that is approximately in equilibrium, so that the subsequent form-finding analysis will produce only minor distortions of the surface. Also, because adjacent gores of the membrane are stressed differently, it must be ensured that any loads applied to the ribs lie within their plane of curvature. This is best done by determining a series of interface equilibrium conditions from which we can obtain initial prestress distributions that satisfy equilibrium in the local, $X_L Y_L$, plane without applying any out-of-plane loads on the ribs.

Consider a general state of prestress of the membrane where each gore is subject to uniform stress and the principal stress directions in gore i are aligned with the local x_i, y_i axes of the gore, Fig. 6. Let t_{xi} and t_{yi} be the values of the principal stress components multiplied by the thickness of the membrane.

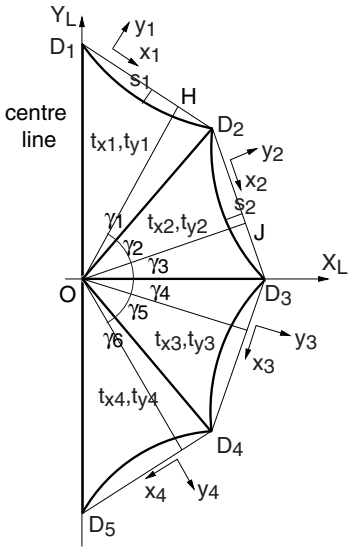

Figure 6: Projection of half of the reflector onto local $X_L Y_L$ plane.

The components of t_{xi} and t_{yi} in the local plane are required to be in equilibrium. This can be achieved either by varying t_{xi}, t_{yi} with i, or by keeping them constant while varying the shape of the gores.

The two-dimensional equilibrium of a shell of general shape can be analysed by considering the projection of the shell onto the plane in which equilibrium is to be considered (Flugge, 1973). Hence, consider, for example, the projection onto the $X_L Y_L$ plane of an offset reflector with eight ribs, shown in Fig. 6. From the centre of the ellipse, O, consider the lines OH, OJ, etc. perpendicular to the edge lines D_1D_2, D_2D_3, etc.

Next, consider the free body consisting of OD_2H and OD_2J, on either side of OD_2, Fig. 7. Similar free bodies can be considered for a general rib, OD_i. By assuming that the ribs apply no external forces to these free bodies one can set up a system of equilibrium equations relating the prestress components in neighboring ribs. Thus, for any given two values, all other values can be worked out.

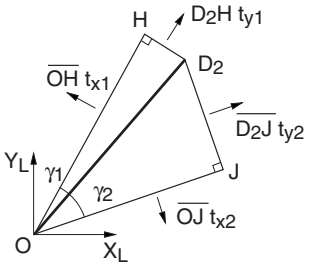

Figure 7: Free body diagram for membrane elements OD_2H and OD_2J.

There is a problem with this approach: it is difficult to produce an acceptable distribution of prestress because the "hoop" and "radial" components of prestress interact through the equilibrium equations at the various interfaces, which often produces unacceptably high, or low stresses in the gores that are furthest away from the gore whose prestress has been specified.

An alternative approach, that has been found to work better, is to assume that each rib is able to carry small longitudinal tractions and hence that equilibrium at each gore-gore interface needs to be enforced only in the direction orthogonal to the rib. To avoid that the hoop stresses be equilibrated by radial stresses, it is required that the x_i components be in equilibrium in the direction orthogonal to the ribs, and it is separately required that the y_i components be independently in equilibrium in the same direction. This gives

$$\begin{aligned} \overline{OH} t_{x1} \cos\gamma_1 - \overline{OJ} t_{x2} \cos\gamma_2 &= 0 \\ \overline{D_2H} t_{y1} \sin\gamma_1 - \overline{D_2J} t_{y2} \sin\gamma_2 &= 0 \end{aligned} \qquad (3)$$

With this approach the prestress components in one gore are prescribed and the components in all the other

gores are computed from equations equivalent to Equation 3.

Note that, although in this approach it is assumed that each rib will be subject to a distribution of longitudinal tractions, in practice these forces would be carried by a narrow strip of membrane in the vicinity of the rib. They cannot be transmitted to the rib because the membrane can slide relative to the rib; they are fully connected only at the tip.

Finally, the edge cord pre-tensions are determined by prescribing the central sag of one gore, e.g. $s_1 = D/15$. It is then assumed that (i) each cord has a symmetric shape, and so the tangent in the middle of cord i is parallel to x_i, and (ii) each rib can carry only axial forces, and hence the tip forces at the points of attachment with the cords are purely in the direction of the rib. Simple equilibrium considerations lead to relationships between the tension in the middle of cord i, T_i, the sag of cord i, s_i, and the sag of cord $i+1$, s_{i+1}, etc. from which all cord pre-tensions can be calculated.

The above considerations illustrate the potential complexity of determining an initial prestress distribution for an offset membrane reflector. If, however, we are prepared to let the shape of the gores vary, the process can be much simplified. Thus, for the "circular configuration" shown in Fig. 4(b), which is again symmetric, the above equilibrium conditions are satisfied by any symmetric distribution of prestress.

Natural Frequency of Vibration

A careful study of the natural frequencies of prestressed membrane structures has been carried out. First, finite-element models of flat membranes with regular shapes were compared to standard, analytical solutions (Kukathasan and Pellegrino, 2002). Then, having shown that the finite element models are accurate for these simple structures, the same methodology was extended to CRTS reflectors. The first few natural frequencies of reflectors of different diameters and numbers of ribs were obtained, and were found to be relatively insensitive to prestress level and hub size.

The fundamental natural frequency of a 10 m diameter reflector was found to be well above 1 Hz. Further details can be found in Kukathasan and Pellegrino (2001).

DESIGN OF PROTOTYPE

A complete design of a 1.5 m diameter offset circular CRTS reflector with focal length of 0.9 m was developed and implemented as a complete structural demonstrator, which was then tested. The properties of this reflector are defined in Table 2 and a front view is shown in Fig. 8.

Diameter (D)	1.5 m
Focal length (F)	0.9 m
F/D	0.6
Offset (A)	0.35 m
Hub diameter	0.15 m
Number of ribs	12
Hoop prestress t_x	40 N/m
Meridional prestress t_y	0.1 N/m
Edge cord sag (s)	$D/100$

Table 2: Properties of prototype.

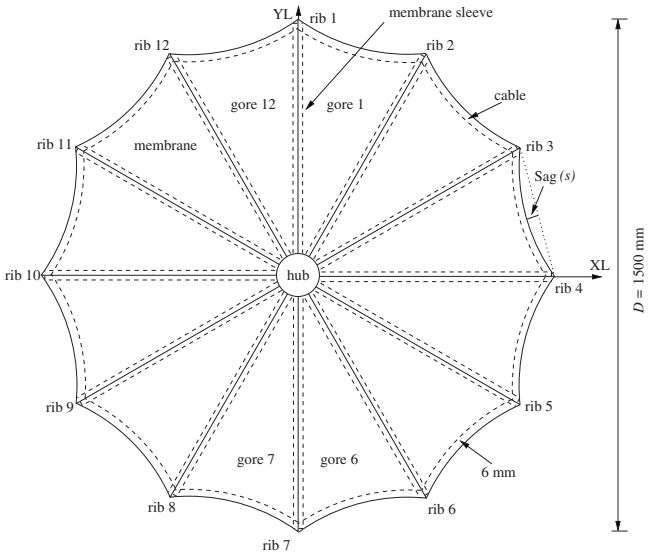

Figure 8: Schematic front view of prototype.

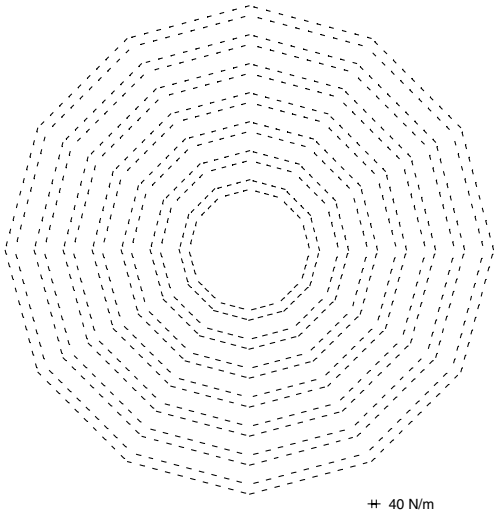

Figure 9: Plot of principal stress directions and magnitudes.

It is often argued that to avoid the formation of wrinkles, thin membranes need to be subjected to equi-biaxial states of prestress. However, the formation of large wrinkles requires either stretching of the membrane (which Kevlar-reinforced Kapton will not do by any significant amount) or the boundary supports to be non-smooth.

Hence it was decided that an essentially uniaxial distribution of prestress, in the hoop direction, would be acceptable. This approach has a number of advantages: (i) the reflector surface can be made from flat, in-plane stiff gores; (ii) the accuracy of the reflector can be easily predicted, as its shape coincides with the reference surface; (iii) the calculation of the cutting patterns for the gores and the analysis of the elastic deformation of the ribs can be done quite accurately by considering simple two-dimensional models.

A hub mechanism design was designed, in which each rib is mounted on a linear bearing and is pulled outwards by a single steel cable that applies a prestressing force, Fig. 10. The ratios between the rib forces, related to the number of ribs, diameter, offset and focal length of the reflector, are controlled by varying the diameter of the pulleys supporting this cable. The whole system is driven by a single electric motor.

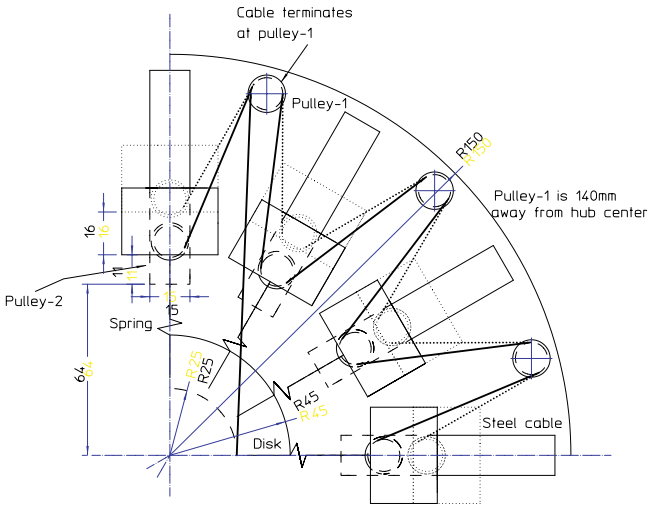

Figure 10: Hub mechanism design (all dimensions are in mm).

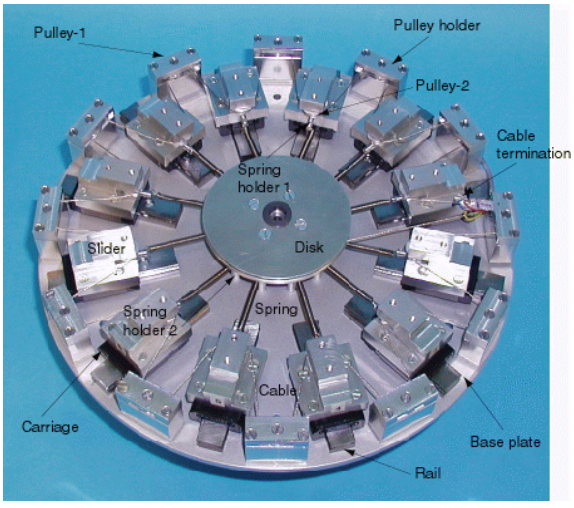

Figure 11: Hub mechanism.

The complete mechanism, shown in Fig. 11, has a mass of ≈ 6 kg and contains a large number of moving parts. Possible changes to make it lighter would be mounting the ribs on springs perpendicular to the plane of the hub, thus removing all the linear bearings, and using a thermally activated shape-memory wire (Nitinol) instead of the steel cable, electric motor, gears and disk.

Rib Design

The ribs are similar to a steel tape measure but have a small longitudinal curvature as well, see Figure 12. The thickness, t, and tranverse radius of curvature R are uniform. They are usually made of either Copper Beryllium (CuBe) or spring steel; CuBe was selected because it can be heat-treated at lower temperature.

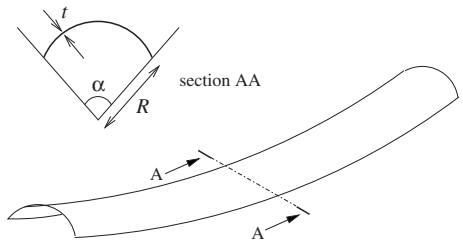

Figure 12: Views of doubly curved rib.

There are two important parameters that need to be considered in deciding the dimensions of the ribs. They are (i) the maximum bending moment that can be applied by the membrane without buckling the rib, and (ii) the yield limit that governs the folding of the rib when the reflector is packaged.

Figure 13 shows a typical relationship between the bending moment, M, and the end rotation, θ, for a short length of rib (Seffen et al., 2000). Note that its behaviour is different for different signs of the bending moment. In the bottom-left-part of the diagram, a negative bending moment applies compressive stresses to the longitudinal edges of the tape spring. In the right-hand-part a positive bending moment is applied, and hence the edge stresses are tensile. Therefore, the buckling moment is much higher for positive moment, i.e. $M^{+}_{max} >> |M^{-}_{max}|$.

Note that for both positive and negative bending, M becomes constant when $|\theta|$ is sufficiently large (typically around 10°). In this range the deformation of the rib is localised in a short, longitudinally curved region and when $|\theta|$ is further increased all that happens is that the length of this curved region increases. In effect, this region behaves like a *constant moment elastic hinge*.

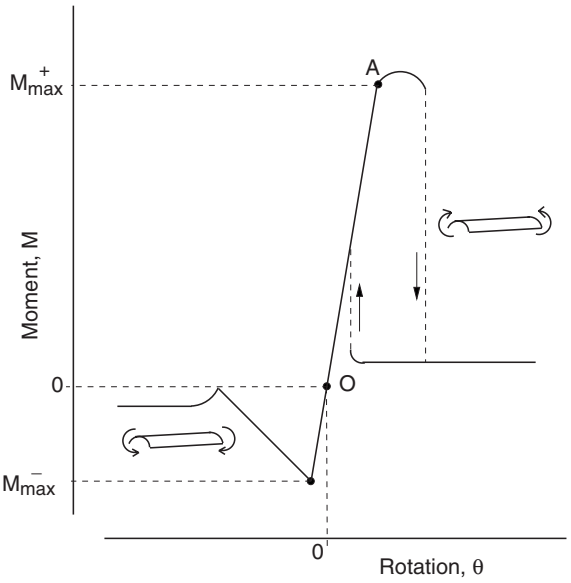

Figure 13: Typical moment-rotation relationship of a rib.

TESTING OF PROTOTYPE

Shape Accuracy

The surface accuracy of the demonstrator was measured with computer controlled electronic theodolites and the RMS error was found to be 2.0 mm; this value is actually *lower* than the predicted value of 2.3 mm.

Folding and Deployment

Following You and Pellegrino (1994) the demonstrator was packaged by wrapping the ribs together with the membrane around a perspex tube attached to the hub. First, each rib was folded upwards towards the perspex tube. Then, the membrane between the ribs was pulled out. At this point, the packaging scheme proposed by You and Pellegrino (1994) would require that all ribs be twisted around the hub until they are fully packaged, but friction between the membrane and the cylinder did not allow this. Three people were required to carry out the packaging, two holding the ribs folded while the third went around the package, gradually bending and twisting one rib at a time towards its final configuration. When the packaged configuration had been finally achieved, an elastic band was put around the structure to hold it folded.

Figure 14 shows the final, packaged configuration. It can be seen that the ribs were not packaged very tightly, especially at the bottom. The height of the package is about 300 mm and its diameter at the bottom is about 450 mm, as the ribs come out about 75 mm on each side. This was the best that could be achieved; it was found that the perspex cylinder does not support well the bent and twisted ribs, and three ribs became damaged. It is believed that a folding machine could simplify this process considerably.

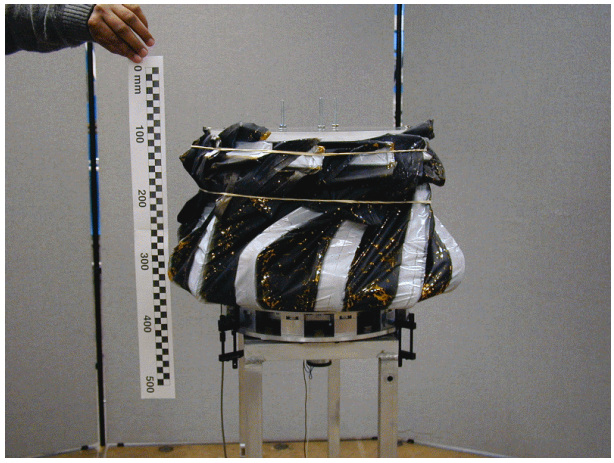

Figure 14: Demonstrator packaged by wrapping.

Figure 15 shows selected frames from the deployment sequence. The time interval between the first 12 frames is 100 ms, increasing to 134 ms for the last four. During the first 400 ms the ribs unwrap, leaving a single fold in each rib, near the hub. Then, between frames 500 ms and 1334 ms, the ribs deploy as cantilever beams connected by hinges to the hub. After 1334 ms all the folds have disappeared and the ribs reach their fully deployed configuration. The remaining frames show a slow oscillation of the structure. In this case, deployment was completed successfully, but the deployment of the twelve ribs was less well coupled than observed by Seffen et al. (2000) on a smaller model. This was probably due to the damage mentioned above.

This test confirmed a conclusion already reached by Seffen et al. (2000), that an advantage of this packaging scheme is that the membrane provides a useful coupling between the motion of the ribs. The correct deployed configuration is always reached, regardless of the orientation of the reflector with respect to gravity.

DISCUSSION

When CRTS reflectors were first proposed, concerns had been expressed over the applicability of this concept to offset configurations. Hence, the key aim of the present study was to investigate the feasibility of offset reflectors, and to develop an appropriate design methodology for them. This aim has been fully achieved.

A special offset configuration has been identified, called a "circular configuration", which makes it possible to practically eliminate any out-of-plane loading on the ribs. This configuration is obtained by intersecting the parent paraboloid with a circular cylinder whose axis is parallel to the local axis Z_L. It has the special feature that the tips of the ribs are not co-planar but, instead, their projections onto the local plane $X_L Y_L$ lie on a circle.

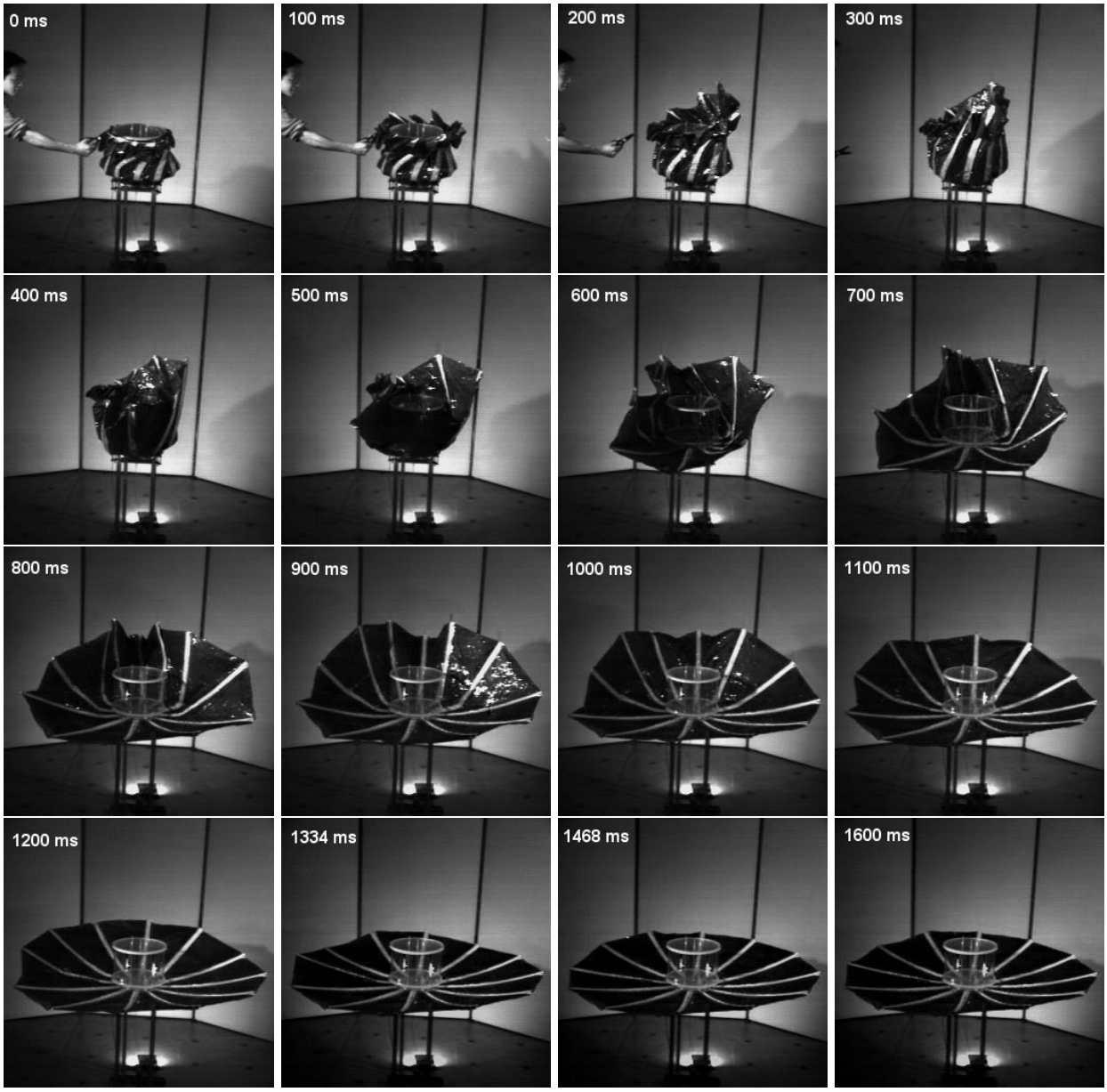

Figure 15: Deployment sequence.

This greatly simplifies the choice of a suitable initial state of prestress because, as far as two-dimensional equilibrium is concerned, this configuration is "axisymmetric" and hence adjacent gores are equally stressed. This solution tends to produce the best distributions of prestress. However, because in this configuration the shape of the reflecting surface does not match the standard illumination pattern for antenna feeds, it is possible that a part of the surface would not be utilised.

The design, manufacture, and testing of a 1.5 m diameter prototype with twelve ribs has been presented, to validate the design methodology developed in this study. The expected root-mean-square surface error of the demonstrator was 2.3 mm and measurements of the actual shape obtained are in excellent agreement. Deployment tests carried out on this structure have confirmed that reliable deployment behaviour is achieved if the reflector is packaged by wrapping the ribs around the hub.

ACKNOWLEDGMENTS

The work presented in this paper was carried out under contract from the European Space Agency. I thank the Project Manager, W.J. Rits, for advice and encouragement, and Drs C.Y. Lai and Z. You for carrying out much of the work summarised in this paper. The Kevlar-reinforced Kapton foil for the prototype was kindly provided by Contraves.

REFERENCES

Flugge, W. (1973). *Stresses in Shells*, Chapter 4. Springer Verlag, Berlin.

Kukathasan, S. and Pellegrino, S. (2001). Vibration of prestressed membrane reflectors, Department of Engineering, University of Cambridge, CUED/D-STRUCT/TR194.

Kukathasan, S. and Pellegrino, S. (2002). Vibration of Prestressed Membrane Structures in Air. 43rd AIAA/ASME/ASCE/AHS/ASC Structures, Structural Dynamics and Materials Conference, 22-25 April 2002, Denver, CO, AIAA 2002-1368.

Lai, C.Y. and Pellegrino, S. (1999). Shape and stress analysis of offset CRTS reflectors. Department of Engineering, University of Cambridge, CUED/D-STRUCT/TR177.

Lai, C.Y., You, Z. and Pellegrino, S. (1998). Shape of deployable membrane reflectors. *Journal of Aerospace Engineering*, **11**, pp. 73-80.

Levy, R. (1996). *Structural Engineering of Microwave Antennas*, Chapter 1. IEEE Press, New York.

Rits, W.J. (1996). A multipurpose deployable membrane reflector. *Esa Bulletin*, **88**, pp. 66-71.

Seffen, K.A., You, Z. and Pellegrino, Z. (2000). Folding and deployment of curved tape springs. *International Journal of Mechanical Sciences*, **42**, pp. 2055-2073.

You, Z. and Pellegrino, S. (1994). Study of the folding and deployment aspects of a Collapsible Rib Tensioned Surface (CRTS) Antenna reflector. Department of Engineering, University of Cambridge, CUED/D-STRUCT/TR 144.